Developmental and Comparative Immunology 52 (2015) 192–201

Contents lists available at ScienceDirect

Developmental and Comparative Immunology

journal homepage: www.elsevier.com/locate/dci

The broad pattern recognition spectrum of the Toll-like receptor in mollusk Zhikong scallop *Chlamys farreri*

Mengqiang Wang [a], Lingling Wang [a], Ying Guo [a], Rui Sun [a], Feng Yue [a], Qilin Yi [a], Linsheng Song [a,b,*]

[a] The Key Laboratory of Experimental Marine Biology, Institute of Oceanology, Chinese Academy of Sciences, 7 Nanhai Rd., Qingdao 266071, China
[b] Dalian Ocean University, Dalian 116023, China

ARTICLE INFO

Article history:
Received 9 April 2015
Revised 22 May 2015
Accepted 22 May 2015
Available online 27 May 2015

Keywords:
Chlamys farreri
Innate immunity
Pattern recognition
Toll-like receptor

ABSTRACT

Toll-like receptors (TLRs) are among the most studied pattern recognition receptors (PRRs) playing essential roles in innate immune defenses. In the present study, the basic features of *Cf*TLR in mollusk Zhikong scallop *Chlamys farreri*, including sequence homology, tissue distribution, subcellular localization and ligands spectrum, were investigated to elucidate its pattern recognition. The elements of extracellular domains (ECD) in *Cf*TLR displayed high homology to the corresponding parts of the ECDs in TLRs from *Homo sapiens*. *Cf*TLR protein was detected in hemocytes, mantle, gills, hepatopancreas, kidney and gonad of the scallops, and it was localized in both the plasma membranes and the lysosomes in HEK293T cells. *Cf*TLR could activate NFκB in response to multiple *Hs*TLR ligands including Pam3CSK4, glucan (GLU), peptidoglycan (PGN), polyriboinosinic:polyribocytidylic acid (poly I:C), Imiquimod and three types of CpG. Additionally, the scallop serum could enhance the induction of NFκB in the *Cf*TLR expressing cells elicited by most PAMPs, including GLU, PGN, Imiquimod and four types of CpG. It could be concluded that this primitive mollusk TLR shared a hybrid function in pattern recognition and could recognize broader ligands than mammalian TLRs, and its mosaic capability of pathogen associated molecular pattern (PAMP) recognition might be based on the basic features of its structure, ligand properties and the assistance of some components in scallop serum.

1. Introduction

The innate immune system acts as the first and unique defense mechanism for invertebrates to protect themselves from invading microbes (Janeway and Medzhitov, 2002). This efficient and complex system employs a set of germ cell encoded receptors termed pattern recognition receptors (PRRs) to recognize the conserved microbial structures termed pathogen associated molecular patterns (PAMPs) (Palm and Medzhitov, 2009). The recognition of various PAMPs by PRRs is the first and pivotal step of innate defense mechanism and can initiate a series of innate immune responses to kill or eliminate invading microbes (Girardin et al., 2002).

In recent years, Toll-like receptors (TLRs) have been recognized as essential PRRs playing pivotal roles in host innate immune defense system (Akira et al., 2001). All TLRs belong to type I membrane receptors and contain leucine-rich repeats (LRRs) motifs in their extracellular domain (ECD) mediating the recognition of PAMPs, a trans membrane domain, and an intracellular Toll/interleukin-1 receptor (TIR) domain required for downstream signal transduction (Bell et al., 2003). After the first *Toll* protein was identified in *Drosophila melanogaster*, TLRs have been described in a great variety of animals and detected in many immune cells including dendritic cells, lymphocytes and macrophages (Matzinger, 2002). Ten and twelve functional TLRs have been identified in human and mice, respectively, with TLR1–TLR9 being conserved in both species (Lee et al., 2012). Among these conserved TLRs, the ones locating in plasma membrane recognize microbial components of cell wall, while others locating in endosome or lysosome participate in the recognition of nucleic acids and their derivatives (Akira et al., 2006). Pattern recognition by TLRs initiates signal transduction pathways via five TIR-domain containing adaptors, followed by the activation of a wide range of inducible transcriptional factors leading to the production of various immune effectors (O'Neill and Bowie, 2007).

Recent genome-wide analyses have revealed a great variety of TLRs or TLR-like genes in the genome of non-mammalian organisms, such as teleost fish, ascidian, amphioxus, shrimps, crab, sea urchin, sea cucumber, squids, mussel and oyster (Arts et al., 2007; Inamori et al., 2004; Mekata et al., 2008; Nyholm and McFall-Ngai, 2004; Ren et al., 2013; Sasaki et al., 2009; Sun et al., 2013; Wei et al., 2011; Yang et al., 2007, 2008; Yuan et al., 2009; Zhang et al.,

* Corresponding author. Dalian Ocean University, 52, Heishijiao Street, Dalian 116023, China. Tel.: +86 532 82898552; fax: +86 532 82880645.
E-mail address: lshsong@dlou.edu.cn (L. Song).

http://dx.doi.org/10.1016/j.dci.2015.05.011
0145-305X/

2011). Furthermore, pattern recognition features of several TLRs or TLR-like genes from non-mammalian animals have been already documented (Coscia et al., 2011). For example, two TLRs from the ascidian *Ciona intestinalis* were reported to display a broader PAMP recognition spectrum than that of TLRs in vertebrates (Sasaki et al., 2009). A TLR from the Chinese amphioxus *Branchiostoma belcheri tsingtauense* (*Bbt*TLR) could be stimulated by bacteria and PAMPs but it could not recognize PAMPs directly (Yuan et al., 2009). A member of the TLR family is involved in dsRNA innate immune response in the sea urchin *Paracentrotus lividus* (Russo et al., 2015). One and three Spätzle-like proteins have been characterized in the shrimps *Fenneropenaeus chinensis* and *Litopenaeus vannamei*, respectively (Shi et al., 2009; Wang et al., 2012), and the mechanism of pattern recognition by TLR in marine crustaceans is considered similar to that in *Drosophila*. In mollusk, four *Cg*TLRs from *Crassostrea gigas* could constitutively activate NFκB responsive reporter in HEK293 cells, but no PAMPs could stimulate *Cg*TLR-activated NFκB induction (Zhang et al., 2013). All these evidences suggested that the pattern recognition mechanism might be diverse in lower animals (Loker et al., 2004). However, only a few evidences on the pattern recognition mechanism and the existence of functional signaling pathway of TLR have been so far accumulated in mollusk.

Zhikong scallop *Chlamys farreri* (Mollusca; Bivalvia; Pteriomorphia) is an important economic bivalve species cultured widely in the northern coast of China. In our previous report, a TLR (*Cf*TLR) and its primitive signaling pathway have been preliminary characterized in *C. farreri*, which could activate downstream anti-bacteria activity, anti-oxidant response and apoptosis process in the immune response against *Vibro anguillarum* (Wang et al., 2011). Investigation on the pattern recognition of *Cf*TLR could provide a better illustration on the functional evolution of TLR signaling pathway in lower animals. The main objectives of the present study are (1) to characterize the sequence homology, tissue distribution and subcellular localization of *Cf*TLR; (2) to screen the ligand spectrum of *Cf*TLR; and (3) to investigate the effect of scallop serum components and ligand properties on the pattern recognition capability of *Cf*TLR, and further to understand the pattern recognition mechanism of *Cf*TLR.

2. Materials and methods

2.1. Animals and immune stimulation

Adult scallops with an average 55 mm in shell length were collected from a local farm in Qingdao, Shandong Province, China, and maintained in the aerated seawater at approximately 15 °C for 2 weeks before processing. The Gram negative bacteria *V. anguillarum* strain M3 (kindly provided by Prof. Zhaolan Mo, Yellow Sea Fisheries Research Institute, Chinese Academy of Fishery Sciences) was cultured in the liquid 2216E media (HB1032-1K, HopeBio, China) at 28 °C to OD_{600} = 0.2 and then centrifuged at 2000 *g* for 5 min to harvest the bacteria. The Gram positive bacteria *Micrococcus luteus* (28001, Microbial Culture Collection Center, Beijing, China) was cultured in the liquid LB media (SD7002, Sangon, China) at 28 °C to OD_{600} = 0.4 and then centrifuged at 2000 *g* for 10 min to harvest the bacteria. The fungus *Yarrowia lipolytica* (kindly provided by Prof. Zhenming Chi, College of Marine Life Science, Ocean University of China) was cultured in the liquid YPD media (SD7022, Sangon, China) at 28 °C to OD_{600} = 0.5 and then centrifuged at 4000 *g* for 10 min to harvest the yeast. All the pellets were re-suspended in filtered seawater and adjusted to 1×10^5 CFU mL^{-1}. Thirty scallops were employed for the microbe stimulation assay by immersion with mixed microorganism at the concentration of 1×10^5 CFU mL^{-1} for 1 week. The hemolymph from the survivors were collected and centrifuged at 800 *g*, at 4 °C for 10 min to harvest the serum. The serum was filtered with a 0.22 μm filter and used for ligand screen assay.

2.2. Homology and similarity analysis

The protein domains and motifs were predicted with the simple modular architecture research tool (SMART) version 7.0 (Letunic et al., 2012). Homology and similarity of *Cf*TLR with TLRs from *Homo sapiens* (designed as *Hs*TLRs) were analyzed via Basic Local Alignment Search Tool (BlastP) (Altschul et al., 1990) and ClustalW programs (Thompson et al., 2002). All *Hs*TLRs sequences were downloaded from NCBI website, including *Hs*TLR1, NP_003254; *Hs*TLR2, NP_003255; *Hs*TLR3, NP_003256; *Hs*TLR4, NP_612564; *Hs*TLR5, NP_003259; *Hs*TLR6, NP_006059; *Hs*TLR7, NP_057646; *Hs*TLR8, NP_619542; and *Hs*TLR9, NP_059138.

2.3. Recombination and purification of Cf*TLR extracellular domain*

The cDNA fragment encoding the ECD of *Cf*TLR was amplified using PrimeSTAR HS DNA polymerase (DR010, Takara, Japan) with specific primers *Cf*TLR-ECD-recombinant-F and *Cf*TLR-ECD-recombinant-R (Table 1). A BamH I site was added to the 5′ end of primer *Cf*TLR-ECD-recombinant-F and a NotI site to the 5′ end of *Cf*TLR-ECD-recombinant-R. The PCR fragments were cloned into p*EASY*-blunt simple vector (CB111, Transgen, China), digested completely by restriction enzymes BamH I HF and Not I HF (R3136 and R3189, NEB, USA), and then cloned into the BamHI/NotI sites of expression vector pET-22b(+) (69744, Novagen, USA) (designed as pET-22b-*Cf*TLR-ECD). The recombinant plasmid pET-22b-*Cf*TLR-ECD was isolated by E.Z.N.A. Plasmid Mini Kit (D6942, Omega, USA) and then transferred into *Escherichia coli* BL21 (DE3) (CB105, Tiangen, China). The positive transformants *E. coli* BL21 (DE3)/pET-22b-*Cf*TLR-ECD were incubated in liquid LB medium containing 100 mg L^{-1} ampicillin at 37 °C with shaking at 220 rpm. When the culture media reached OD_{600} of approximately 0.4–0.6, the cells were incubated for 4 additional hours with the induction of isopropyl β-D-1-thiogalactopyranoside (IPTG, 776687, AiKB, China) at the final concentration of 1 mmol L^{-1}. The recombinant protein r*Cf*TLR-ECD was purified by a Ni^{2+} chelating Sepharose column (71–5027-67, Novagen, USA) under denatured condition (8 mol L^{-1} urea). The purified protein was refolded in gradient urea–TBS glycerol buffer (50 mmol L^{-1} Tris–HCl, 50 mmol L^{-1} sodium chloride, 10% glycerol, 2 mmol L^{-1} reduced glutathione, 0.2 mmol L^{-1} oxide glutathione, a gradient urea concentration of 6, 5, 4, 3, 2, 1 and 0 mol L^{-1} urea, pH 8.0; each gradient at 4 °C for 12 h). The purified products were subjected to 15% sodium dodecyl sulphate–polyacrylamide gel electrophoresis (SDS–PAGE) and then visualized by coomassie brilliant blue R-250 staining. The concentration of purified recombination proteins was quantified via an Enhanced BCA Protein Assay Kit (P0010, Beyotime, China), and the obtained proteins were stored at –80 °C before use.

2.4. Preparation of antibody and western blotting analysis

For preparation of antibodies, the re-natured protein r*Cf*TLR-ECD was continued to be dialyzed against ddH_2O before it was freeze concentrated. r*Cf*TLR-ECD was immunized to 6-week old rats to acquire polyclonal antibody using the water soluble adjuvant QuickAntibody (KX0210043, KBQbio, China) according to the manufacturer's directions. The blood of the immunized rat was collected from the heart and allowed to clot at 4 °C overnight. The clotted blood was centrifuged at 3000 *g* for 20 min and the serum was tested via western blotting according to previous reports and used as antibody against *Cf*TLR protein (Guo et al., 2013).

Table 1
Brief information of primers used in current research.

Name	Sequence(5′–3′)	Primer information
*Cf*TLR-ECD-recombinant-F	GGATCCGGTTGAGTACACGTGCCCCGAAGAA	Prokaryotic recombinant
*Cf*TLR-ECD-recombinant-F	GCGGCCGCCGGGCGATTGTCCGTGCGGTC	Prokaryotic recombinant
*Cf*TLR-CDS-infusion-F	CGGACTCAGATCTCGAGCTCACCATGGCGCGGCCAACGTGTGTTGTC	Mammalian expression
*Cf*TLR-CDS-infusion-R	GTGGATCCCGGGCCCGCGGAGCCATTTGCTTCTCTGATTTTTC	Mammalian expression
*Cf*TLR-CDS-recombinant-F	AGGATGGCGCGGCCAACGTGTGTTGTC	Mammalian expression
*Cf*TLR-CDS-recombinant-R	AGCCATTTGCTTCTCTGATTTTTC	Mammalian expression
*Cf*MyD88-CDS-recombinant-F	AGGATGGCAATGGCGGATATCGAG	Mammalian expression
*Cf*MyD88-CDS-recombinant-R	CTCTCCTCGTTTTTTATTTTTGTT	Mammalian expression
*Cf*TLR-ΔICD-infusion-F	CGAATGCATCTAGATATCATGACGCGGCCAACGTGTGTTGTC	Mosaic palsimid
*Cf*TLR-ΔICD-infusion-R	CCAAAACGCCAGACCAAGAGCAAC	Mosaic palsimid
*Hs*TLR1-ICD-infusion-F	GGTCTGGCGTTTTGGGATCTGCCCTGGTATCTCAGGATG	Mosaic palsimid
*Hs*TLR1-ICD-infusion-R	GGCCCGGATCCGATATCCTATTTCTTTGCTTGCTCTGTCAGCTT	Mosaic palsimid
*Hs*TLR2-ICD-infusion-F	GGTCTGGCGTTTTGGCGTTTCCATGGCCTGTGGTATATG	Mosaic palsimid
*Hs*TLR2-ICD-infusion-R	GGCCCGGATCCGATATCCTAGGACTTTATCGCAGCTCTCAG	Mosaic palsimid
*Hs*TLR3-ICD-infusion-F	GGTCTGGCGTTTTGGGAGGGCTGGAGGATATCTTTTTATTGG	Mosaic palsimid
*Hs*TLR3-ICD-infusion-R	GGCCCGGATCCGATATCTTAATGTACAGAGTTTTTGGATCCAAGTGC	Mosaic palsimid
*Hs*TLR4-ICD-infusion-F	GGTCTGGCGTTTTGGCACCTGATGCTTCTTGCTGGCTGC	Mosaic palsimid
*Hs*TLR4-ICD-infusion-R	GGCCCGGATCCGATATCTCAGATAGATGTTGCTTCCTGCCA	Mosaic palsimid
*Hs*TLR5-ICD-infusion-F	GGTCTGGCGTTTTGGTGTTTTATCTGTTATAAGACAGCCCAGAGA	Mosaic palsimid
*Hs*TLR5-ICD-infusion-R	GGCCCGGATCCGATATCTTAGGAGATGGTTGCTACAGTTTGCAA	Mosaic palsimid
*Hs*TLR6-ICD-infusion-F	GGTCTGGCGTTTTGGGCACCAAGCACATTCAAGTTTTTGAAC	Mosaic palsimid
*Hs*TLR6-ICD-infusion-R	GGCCCGGATCCGATATCTTAAGATTTCACATCATTGTTTTCAGTGAC	Mosaic palsimid
*Hs*TLR7-ICD-infusion-F	GGTCTGGCGTTTTGGGATGTGTGGTATATTTACCATTTCTGT	Mosaic palsimid
*Hs*TLR7-ICD-infusion-R	GGCCCGGATCCGATATCCTAGACCGTTTCCTTGAACACCTG	Mosaic palsimid
*Hs*TLR8-ICD-infusion-F	GGTCTGGCGTTTTGGCACCATTTGTTTTACTGGGATGTTTGG	Mosaic palsimid
*Hs*TLR8-ICD-infusion-R	GGCCCGGATCCGATATCTTAGTATTGCTTAATGGAATCGACATACAT	Mosaic palsimid
*Hs*TLR9-ICD-infusion-F	GGTCTGGCGTTTTGGCGGGGGCGGCAAAGTGGG	Mosaic palsimid
*Hs*TLR9-ICD-infusion-R	GGCCCGGATCCGATATCCTATTCGGCCGTGGGTCC	Mosaic palsimid
*Hs*TLR1-CDS-recombinant-R	TTTCTTTGCTTGCTCTGTCAGCTT	Mammalian expression
*Hs*TLR2-CDS-recombinant-R	GGACTTTATCGCAGCTCTCAGATT	Mammalian expression
*Hs*TLR3-CDS-recombinant-R	ATGTACAGAGTTTTTGGATCCAAGTGC	Mammalian expression
*Hs*TLR4-CDS-recombinant-R	GATAGATGTTGCTTCCTGCCAATT	Mammalian expression
*Hs*TLR5-CDS-recombinant-R	GGAGATGGTTGCTACAGTTTGCAA	Mammalian expression
*Hs*TLR6-CDS-recombinant-R	AGATTTCACATCATTGTTTTCAGTGAC	Mammalian expression
*Hs*TLR7-CDS-recombinant-R	GACCGTTTCCTTGAACACCTG	Mammalian expression
*Hs*TLR8-CDS-recombinant-R	GTATTGCTTAATGGAATCGACATACAT	Mammalian expression
*Hs*TLR9-CDS-recombinant-R	TTCGGCCGTGGGTCCCTG	Mammalian expression
M13F	GTAAAACGACGGCCAGT	Vector primer
M13R	CAGGAAACAGCTATGAC	Vector primer
T7	TAATACGACTCACTATAGGG	Vector primer
T7 ter	TGCTAGTTATTGCTCAGCGG	Vector primer
EGFP-N sequencing primer	CGTCGCCGTCCAGCTCGACCAG	Vector primer
EGFP-C sequencing primer	CATGGTCCTGCTGGAGTTCGTG	Vector primer
CMV forward	CGCAAATGGGCGGTAGGCGTG	Vector primer
TK PolyA reverse	CTTCCGTGTTTCAGTTAGC	Vector primer

2.5. Immunofluorescence detection of TLR in tissues

Slides of hemocytes were prepared according to the previous report (Guo et al., 2013). The adductor muscle, mantle, gill, hepatopancreas, kidney and gonad of scallops were dissected and fixed with Bouin's fixative for 24 h. The fixed tissues were rinsed, dehydrated and embedded in paraffin wax. Continuous 5 μm thick sections of each embedded specimens were cut using an RM2016 microtome (Leica, German) and mounted on slides. The slides were deparaffined in xylene, washed in PBS-T (0.5% Tween-20 in PBS), and then antigen retrieval was performed via heating in water bath at 120 °C for 6 min. The slides were blocked by incubating in PBS containing 3% BSA at 37 °C for 1 h. After three times washing with PBS-T, the hemocytes and tissue slides were covered with 20 μL antibody raised against r*Cf*TLR (diluted 1:1000 in PBS) as primary antibody and incubated at 37 °C for 1 h in a moisture chamber. The slides were then washed three times with PBS-T and incubated at 37 °C for 1 h with Alexa-488 conjugated goat-anti-rat immunoglobulin serum (A11006, Thermofisher/Life Technologies, USA) diluted at 1:1000 with PBS, containing 1 μg mL^{-1} Evan's blue dye (E2129, Fluka, USA) as the counterstain. Finally, the slides were washed three times and mounted in buffered glycerin for observation by fluorescence microscope. Rat pre-immune serum was used as negative control.

2.6. Mammalian expression vector

To investigate the subcellular localization of *Cf*TLR in human HEK293T cell lines, the cDNA fragment encoding the full coding region of *Cf*TLR was amplified using PrimeSTAR HS DNA polymerase with specific primers *Cf*TLR-CDS-infusion-F and *Cf*TLR-CDS-infusion-R (Table 1) and inserted into expression vector pEGFP-N1 (PT3027, Clontech, USA) (designed as pEGFP-N1-*Cf*TLR) via In-Fusion HD Cloning Kit (636912, Clontech, USA). For the expression of *Cf*TLR and *Cf*MyD88 in HEK293T cells, the full coding regions of *Cf*TLR and *Cf*MyD88 were amplified using the primer of *Cf*TLR-CDS-recombinant-F/R and *Cf*MyD88-recombinant-F/R, separately (Table 1), and then ligated to the pcDNA3.1(+) original mammalian expression vectors p*EASY*-M1 and p*EASY*-M2 (CM101 and CM111, Transgen, China) (designed as p*EASY*-M1-*Cf*TLR and p*EASY*-M2-*Cf*MyD88), respectively. Mosaic vectors p*EASY*-M1-Mosaic1, 2, 3, 4, 5, 6, 7, 8 and 9, in which the *Cf*TLR extracellular and transmembrane domains fused with the intracellular domains of *Hs*TLR1, 2, 3, 4, 5, 6, 7, 8 and 9 (kindly provided by Prof. Jiahuai Han, School of Life Sciences,

Xiamen University) separately, were constructed via In-Fusion HD Cloning Kit and ligated to p*EASY*-M1 vector. All the mammalian expression vectors were isolated by Endo Free Plasmid Maxi Preparation Kit (D0029, Beyotime, China) and stored at –20 °C before use.

2.7. Cell culture and transfection

HEK293T cells (GNHu17, Cellbank of Chinese Academy of Science, China) were maintained in Dulbecco's modified Eagle's medium (DMEM) (11995-065, Thermofisher/Life Technologies, USA) supplemented with 10% heat-inactivated fetal bovine serum (FBS) (10099-141, Thermofisher/Life Technologies, USA) at 37 °C in a humidified atmosphere of 5% carbon dioxide. The cells were transfected using Lipofectamine LTX Reagent (15338-100, Thermofisher/Life Technologies, USA) with the mammalian expression plasmids mentioned earlier according to the manufacturer's directions.

2.8. Subcellular localization assay via confocal microscopy observation

The EGFP-tagged *Cf*TLR transient transfectants were seeded onto glass bottom culture dishes (801001, NEST, China). After adhering for 24 h, the cells were treated with 1,1′-dioctadecyl-3,3,3′,3′-tetramethylindocarbocyanine perchlorate (DiI, C1036, Beyotime, China) or DND 99 labeled Lyso-Tracker Red (C1046, Beyotime, China) according to the manufacturer's directions, and then confocal imaging was carried out utilizing a LSM 710 laser scanning confocal microscope (Carl Zeiss, German).

2.9. Ligand screen assay based on dual luciferase reporter gene assay

For TLR ligand screen assay, HEK293T cells, which do not express TLRs, were plated in 48-well plates (3548, Corning/Costar, USA) (5×10^4 cells per well) and transfected on the following day with approximately 310 ng plasmid DNA per well. The mixed DNA contained 200 ng indicated plasmid together with 100 ng NFκB response promoter luciferase reporter plasmid pNFκB-luc (D0206, Beyotime, China) and 10 ng Renilla luciferase control reporter vector pRL-TK (E2241, Promega, USA). At 24 h post transfection, lipopolysaccharides from *E. coli* 0111:B4 (LPS, 1 μg mL^{-1}, L2630, Sigma-Aldrich, USA), peptidoglycan from *Staphylococcus aureus* (PGN, 1 μg mL^{-1}, 77140, Sigma-Aldrich, USA), β-Glucan from *Saccharomyces cerevisiae* (GLU, 1 μg mL^{-1}, 89863, Sigma-Aldrich, USA), Pam2CSK4 (1 μg mL^{-1}, tlrl-pam2s-1, Invivogen, USA), Pam3CSK4 (1 μg mL^{-1}, tlrl-pms, Invivogen, USA), Imiquimod (5 μg mL^{-1}, tlrl-imq, Invivogen, USA), Zymosan (25 μg mL^{-1}, ZB4250, Sangon, China), polyinosinic–polycytidylic acid (poly I:C, 25 μg mL^{-1}, P1530, Sigma-Aldrich, USA), different type of sulphureted CpG (100 nmol L^{-1}, Sangon, China) (Table 2) or antiserum against *Cf*TLR-ECD (diluted 1:100) were added to cell media, respectively, and then the cells were incubated for additional 12 h at 37 °C. Luciferase activities were assayed via GloMax-20/20 Single Tube Luminometer (Promega, USA) with Dual-Luciferase Reporter Assay Kit (E1910, Promega, USA) and expressed as the fold stimulation relative to the same vector transfected cells incubated without stimulation. The dual luciferase reporter gene assay with scallop serum was similar with the description earlier with scallop serum in the culture media at a final concentration of 5%.

2.10. Statistical analysis

All data were given as means ± S.D. (n = 5). The data were subjected to one-way analysis of variance (one-way ANOVA) followed by a multiple comparison (S-N-K) via IBM SPSS Statistics software version 22.0, and the *p* values less than 0.05 were considered statistically significant.

Table 2
TLR ligands screened in current research.

Ligand	Information	*Hs*TLR
Pam3CSK4	A synthetic triacylated lipopeptide	TLR1/TLR2
1,3-β-Glucan	Laminarin	TLR2
Zymosan	*Sacchromyces cerevisiae* cell wall	TLR2
Peptidoglycan	A major component in outer wall of bacteria	TLR2
Pam2CSK4	A synthetic biacylated lipopeptide	TLR2/TLR6
Polyinosinic–polycytidylic acid	Double-stranded RNA	TLR3
Lipopolysaccharide	A major component in outer wall of bacteria	TLR4
Imiquimod	An imidazoquinolone amino acid analog to guanosine	TLR7
C type CpG	A synthetic oligonucleotide containing sulphureted unmethylated CpG dinucleotide 5′-TCGTCGTTCGAACGACG TTGAT-3′	TLR9
D type CpG	A synthetic oligonucleotide containing sulphureted unmethylated CpG dinucleotide 5′-GGTGCATCGATGCAGGG GGG-3′	TLR9
K type CpG	A synthetic oligonucleotide containing sulphureted unmethylated CpG dinucleotide 5′-TCCATGGACGTTCCTGAG CGTT-3′	TLR9
P type CpG	A synthetic oligonucleotide containing sulphureted unmethylated CpG dinucleotide 5′-TCGTCGACGATCGGCGCG CGCCG-3′	TLR9

3. Result

3.1. Sequence homology of *Cf*TLR with TLRs from H. sapiens

The component parts of ECD from *Cf*TLR displayed high homology to the corresponding parts of the ECDs in *Hs*TLRs (Table 3). For example, the amino acids at 125–577 in *Cf*TLR-ECD were similar to

Table 3
Sequence similarity of extracellular domain in *Cf*TLR to those in *Hs*TLRs.

Amino acid in *Cf*TLR-ECD	Hits of amino acid in *Hs*TLRs	Score	Expect
103–616	*Hs*TLR7, 280–794	62.8	5.0E–14
125–577	*Hs*TLR9, 111–555	71.6	9.0E–17
126–632	*Hs*TLR4, 61–621	61.2	9.0E–14
127–582	*Hs*TLR7, 194–714	57.8	2.0E–12
192–496	*Hs*TLR3, 192–663	60.8	2.0E–13
197–559	*Hs*TLR2, 62–452	51.6	9.0E–11
216–577	*Hs*TLR7, 105–576	64.3	2.0E–14
222–630	*Hs*TLR9, 348–785	63.2	4.0E–14
226–613	*Hs*TLR5, 86–421	55.5	6.0E–12
226–621	*Hs*TLR8, 278–788	53.9	3.0E–11
240–597	*Hs*TLR3, 56–408	53.9	2.0E–11
240–849	*Hs*TLR9, 68–687	53.2	5.0E–11
287–780	*Hs*TLR5, 18–538	69.7	2.0E–16
306–577	*Hs*TLR5, 311–579	54.3	1.0E–11
335–616	*Hs*TLR5, 292–594	57.0	2.0E–12
384–577	*Hs*TLR9, 68–254	60.8	2.0E–13
419–582	*Hs*TLR4, 28–190	58.5	7.0E–13
427–806	*Hs*TLR3, 53–393	52.8	4.0E–11

those at 111–555 in *Hs*TLR9-ECD, while the fragment from 287 to 780 in *Cf*TLR displayed high homology to those at 18–538 in *Hs*TLR5-ECD. However, no parts of *Cf*TLR-ECD exhibited significant homology to those of *Hs*TLR1-ECD or *Hs*TLR4-ECD.

3.2. Recombinant protein of CfTLR-ECD and western blotting analysis

After IPTG induction, the whole cell lysate of *E. coli* BL21 (DE3)/pET-22b-*Cf*TLR-ECD was analyzed by SDS–PAGE, and a distinct band with molecular weight of approximately 110 kDa was revealed, which was consistent with the predicted molecular mass (Fig. 1, line P). The purified protein was used for the preparation of antibody. Western blotting was carried out to identify the specificity of antibody. A clear reaction band with high specificity was revealed, and few non-specific bands were visible (Fig. 1, line W). As the negative control, no visible reaction band was detected in group of rats' pre-immuned serum (data not show).

3.3. Immunofluorescence detection of CfTLR in tissues

The localization of endogenous *Cf*TLR protein was investigated by the method of immunofluorescence, and the green fluorescence signal exhibited the localization of *Cf*TLR. *Cf*TLR was detected in hemocytes (Fig. 2a), mantle (Fig. 2c), gills (Fig. 2d), hepatopancreas (Fig. 2i), kidney (Fig. 2j) and gonad (Fig. 2k) of the scallops. No fluorescence staining was observed in adductor muscle (Fig. 2b). There was no signal in negative control groups (Fig. 2e–h, l–n).

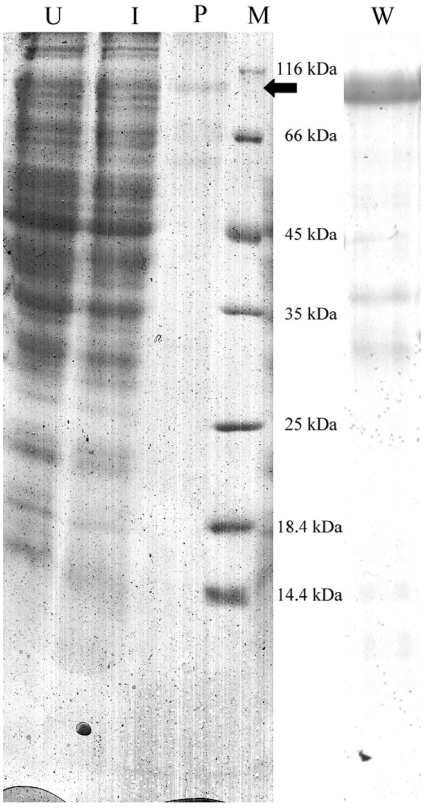

Fig. 1. SDS–PAGE and western blotting analysis of r*Cf*TLR-ECD protein. Lane U: bacteria lysate without induction; lane I: bacteria lysate induced with IPTG; lane P: purified r*Cf*TLR-ECD protein; lane M: protein molecular standard (26610, Thermofisher/Fermentas, USA); lane W: specific of the antiserum tested with western blotting.

3.4. Subcellular localization of CfTLR

To verify the subcellular localization of *Cf*TLR, a double immunofluorescence confocal microscopy observation of the EGFP-tagged *Cf*TLR transient expressed in HEK293T cells was performed. Moreover, DiI and Lyso-Tracker Red were employed as the markers of plasma and lysosome, respectively. Intriguingly, unlike any human and mice TLRs, *Cf*TLR was found to be present in both the plasma membrane and lysosomes (Fig. 3).

3.5. Representative ligands of CfTLR

After the stimulation with antiserum against *Cf*TLR-ECD, neither the solo-transfection of *Cf*TLR nor its co-transfection with *Cf*MyD88 could activate the NFκB luciferase reporter in HEK293T cells (Fig. 4). However, most of the Mosaic vectors could induce the NFκB promoter dependent reporter after the stimulation with antiserum against *Cf*TLR-ECD (Fig. 4). The Mosaic2 vector with the *Cf*TLR extracellular and transmembrane domain fused with the intracellular domain of *Hs*TLR2 was selected to elucidate ligand spectrum of *Cf*TLR according to the results of the present study and a previous report (Yuan et al., 2009). HEK293T cells, which do not express TLRs, were transient transfected with empty pcDNA3.1(+) vector or Mosaic vector p*EASY*-M1-Mosaic2, and treated with 12 known mammalian TLR ligands (Table 2) at the previously verified concentrations that could significantly activate the respective *Hs*TLRs. Unexpectedly, *Cf*TLR could respond to multiple mammalian TLR ligands, such as Pam3CSK4 for *Hs*TLR1/*Hs*TLR2 (Fig. 5a), GLU for *Hs*TLR2 (Fig. 5b), PGN for *Hs*TLR2 (Fig. 5d), poly I:C for *Hs*TLR3 (Fig. 5f) and Imiquimod for *Hs*TLR7 (Fig. 5h). In contrast, there were no significant responses to these ligands in the empty vector-transfected cells compared with the non-transfected cells. While other ligands, including Zymosan for *Hs*TLR2 (Fig. 5c), Pam2CSK4 for *Hs*TLR2/*Hs*TLR6 (Fig. 5e), LPS for *Hs*TLR4 (Fig. 5g), and D-type CpG for TLR9 (Fig. 5j), failed to induce NFκB transactivation in *Cf*TLR transfected cells.

Intriguingly, the scallop serum could enhance the induction of NFκB in the *Cf*TLR expressing cells elicited by most PAMPs, including GLU (Fig. 5b), PGN (Fig. 5d), Imiquimod (Fig. 5h), and four types of CpG (Fig. 5i, 5j, 5k, and 5l). In contrast, the induction of NFκB in the *Cf*TLR expressing cells elicited by Pam3CSK4 (Fig. 5a) and polyinosinic–polycytidylic acid (Fig. 5f) was depressed by scallop serum. Additionally, the NFκB transactivation in the *Cf*TLR expressing cells could be induced by C, K and P-type CpG in normal condition (Fig. 5i, 5k and 5l), and the scallop serum could enhance such induction. Conversely, the D-type CpG even failed to induce NFκB transactivation in *Cf*TLR transfected cells in the absence of scallop serum.

4. Discussion

The innate immune system plays pivotal roles in the defensive responses against invading pathogens in invertebrates where the adaptive immunity is absent (Janeway and Medzhitov, 2002). Although a great variety of TLRs or TLR-like genes have been identified in the genome of invertebrates, little evidence on the functional TLR signaling pathways and their pattern recognition feature have been so far accumulated in mollusk. To address this issue, the present research focused on the characterization of *Cf*TLR structural features, screening of its ligand spectrum, and the effects of ligand properties and scallop serum components on pattern recognition of *Cf*TLR.

So far, ten and twelve functional TLRs have been identified in human and mice, respectively, with TLR1–TLR9 being conserved in both of them (Lee et al., 2012). In the present study, BlastP and ClustalW programs were employed to analyze the homology and similarity of *Cf*TLR with *Hs*TLRs, and the elements of *Cf*TLR-ECD were

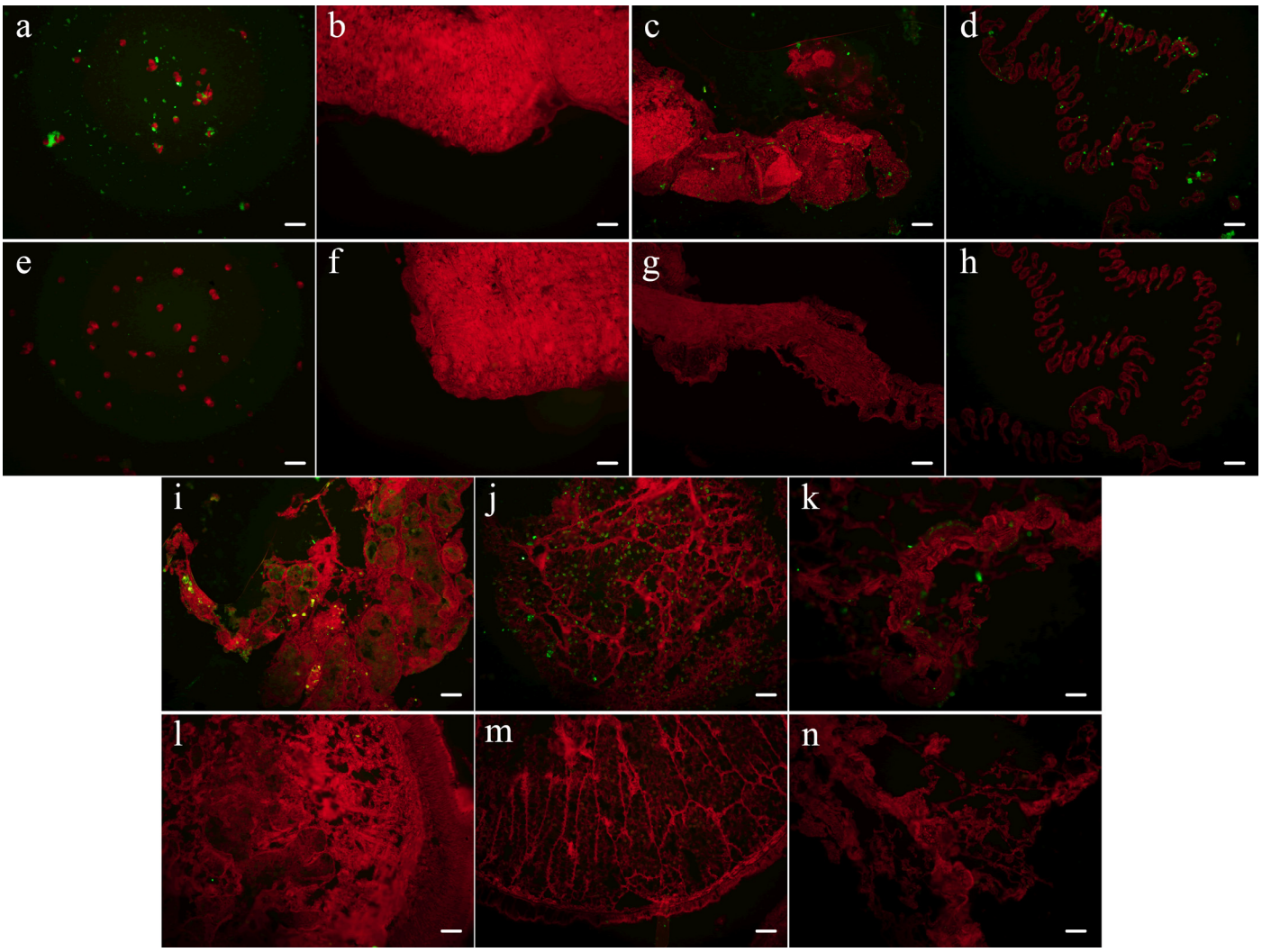

Fig. 2. Localization of endogenous *Cf*TLR in different tissues. Hemocytes or sections of tissues were fixed and then incubated with rat polyclonal antiserum. Binding of antibody was visualized by Alexa-488 conjugated goat-anti-rat immunoglobulin serum (green), and the whole tissues were stained with Evan's blue dye (red). (a and e) Hemocytes, (b and f) muscle, (c and g) mantle, (d and h) gill, (i and l) hepatopancreas, (j and m) kidney, (k and n) gonad; bar = 10 μm. (For interpretation of the references to color in this figure legend, the reader is referred to the web version of this article.)

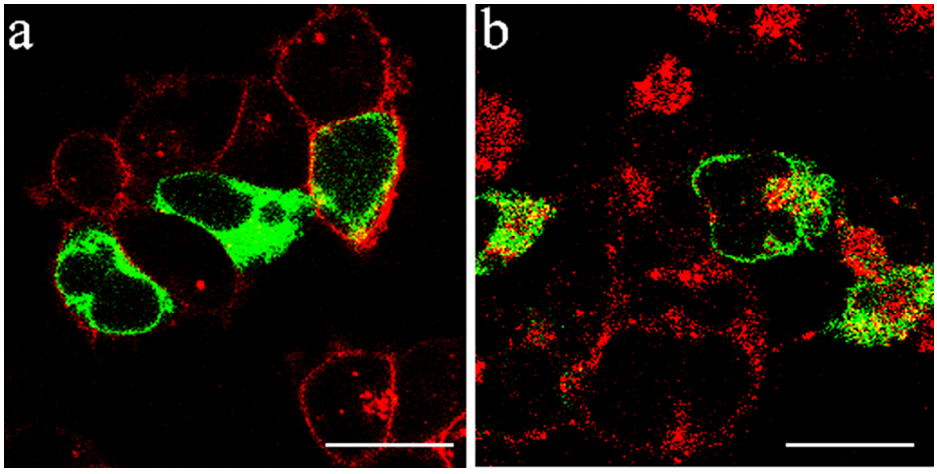

Fig. 3. Cellular localization of *Cf*TLR in HEK293T cells. *Cf*TLR was tagged with EGFP (green), while plasma and lysosome were visualized via DiI (red) and Lyso-Tracker (red), separately; bar = 10 μm. (For interpretation of the references to color in this figure legend, the reader is referred to the web version of this article.)

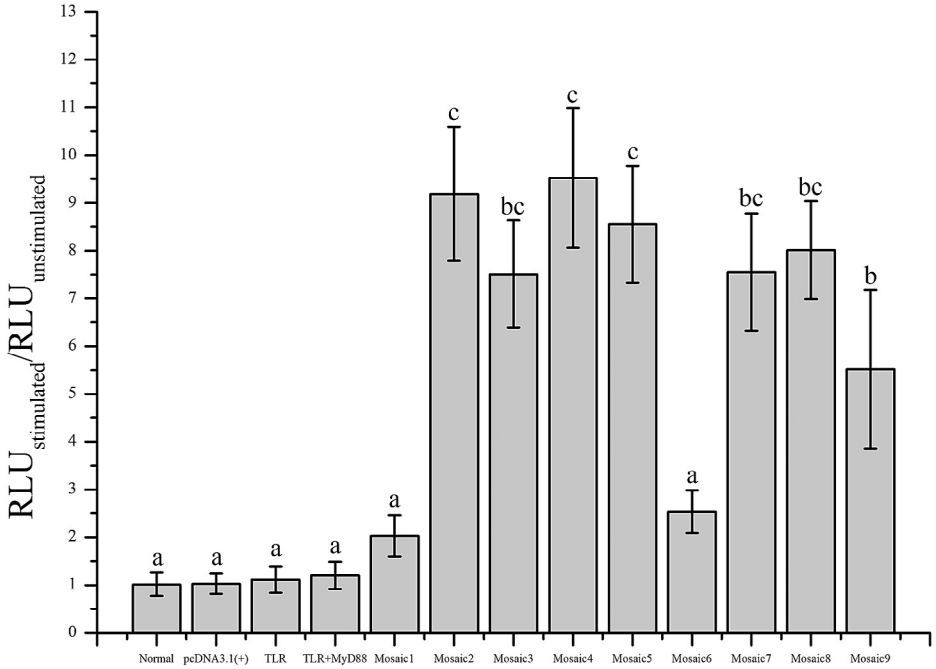

Fig. 4. Dual luciferase report assay of different plasmids. The pcDNA3.1 (+) transfected cells served as negative control, and the pRL-TK Renilla luciferase vector was used as an internal control. The luciferase activities encoded by pNFκB-luc reporter vector were detected. Data were normalized to the value of normal group. Vertical bars represented mean ± S.D. (n = 5), and bars with different characters indicated significantly different ($p < 0.05$).

found to be high homologous to the corresponding parts of *Hs*TLR-ECDs (Table 3). However, there was no element in *Cf*TLR-ECD exhibiting significant homology to those of *Hs*TLR1-ECD or *Hs*TLR4-ECD. Similar with the research achievements in *Ci*TLR1 and *Ci*TLR2 (Sasaki et al., 2009), the mosaic homology and similarity of *Cf*TLR-ECD to corresponding parts of *Hs*TLR-ECDs were the structural foundation for the hybrid function of *Cf*TLR in pattern recognition.

The localization of PRRs is an essential factor affecting their pattern recognition ability of PAMPs (Watts, 2008). Among the conserved mammal TLRs, the ones locating in plasma membrane recognize microbial pathogenic components of cell wall, while the others locating in endosomes or lysosome recognize nucleic acids and their derivatives (Akira et al., 2006). In the present research, *Cf*TLR protein could be detected in most tested tissues, including hemocytes, mantle, gills, hepatopancreas, kidney and gonad, except adductor muscle. Such constitutive expression in various tissues contributed an opportunity for *Cf*TLR to interact with many kinds of PAMPs. Moreover, the double immunofluorescence confocal microscopy observation revealed that *Cf*TLR was localized in both the plasma membranes and the lysosomes, which was obviously different from vertebrate TLRs. Similar cellular localization was also reported for *Ci*TLR1 and *Ci*TLR2 (Sasaki et al., 2009). Although the exact mechanism of such multiple cellular localizations still awaits further study, the localization of *Cf*TLR at both the plasma membranes and the lysosomes allows *Cf*TLR to recognize not only different microbial pathogenic components of cell wall but also nucleic acids and their derivatives into the cytoplasm.

The TLRs from human and mice could be divided into two families, one recognizing microbial components of cell wall and the other participating in pattern recognition of nucleic acids and their derivatives, according to their ligand spectrum (Akira et al., 2006). In the present research, dual luciferase reporter gene assay was employed to screen the ligand spectrum of *Cf*TLR. Neither the solo-transfection of *Cf*TLR nor its co-transfection with *Cf*MyD88 could activate the NFκB luciferase reporter in HEK293T cells (Fig. 4), while most of the Mosaic vectors could induce the NFκB promoter dependent reporter after the stimulation by antiserum raised against *Cf*TLR-ECD (Fig. 4), indicating that the TLR and MyD88 from *C. farreri* could not directly utilize other components of this pathway in HEK293T cells. However, four *C. gigas* TLRs were recently reported to activate NFκB luciferase reporter in HEK293 cells directly (Zhang et al., 2013), suggesting the complexity and variety of TLR signaling pathway in invertebrates. In the present study, the Mosaic2 vector, constructed by the *Cf*TLR extracellular and transmembrane domains with the *Hs*TLR2 intercellular domain, was selected to elucidate the PAMPs recognized by *Cf*TLR. Unexpectedly, *Cf*TLR was found to activate NFκB reporter gene in response to multiple ligands specifically recognized by different mammalian TLRs, including Pam3CSK4 for *Hs*TLR1/*Hs*TLR2, GLU for *Hs*TLR2, PGN for *Hs*TLR2, poly I:C for *Hs*TLR3, Imiquimod for *Hs*TLR7, and some CpGs for *Hs*TLR9, which was consistent with the structural feature of *Cf*TLR in a certain extent. For example, LPS recognized by *Hs*TLR4 failed to induce NFκB transactivation in *Cf*TLR transfected HEK293T cells and no parts of *Cf*TLR-ECD exhibited significant homology to those of *Hs*TLR4-ECD. These results collectively suggested that *Cf*TLR was a functionally mosaic TLR of the two conserved TLR families in pattern recognition. However, it was reported that the *Cg*TLR-activated NFκB induction could not be stimulated by PAMPs in HEK293 cells (Zhang et al., 2013). Considering that all the four *Cg*TLRs investigated in the previous report belonged to multiple cysteine cluster TLRs (mccTLRs), while the *Cf*TLR belonged to single cysteine cluster TLRs (sccTLRs) according to the number of cysteine cluster on the C-terminal end of LRR domains (Leulier and Lemaitre, 2008), it was suggested that the pattern recognition capability of TLRs might mainly be based on their structure feature in invertebrates, and *Cf*TLR could recognize broader ligands than mammalian TLRs.

Unlike mammal TLRs, invertebrate TLRs, for example *Toll* from *Drosophila*, could not directly recognize the PAMPs and they employ the cytokine-like molecule Spätzle as an assistant (Lemaitre et al., 1996). Some Spätzle-like proteins have already been identified and characterized in shrimps, indicating that the pattern recognition mechanism of TLR in crustacean might be similar with that in

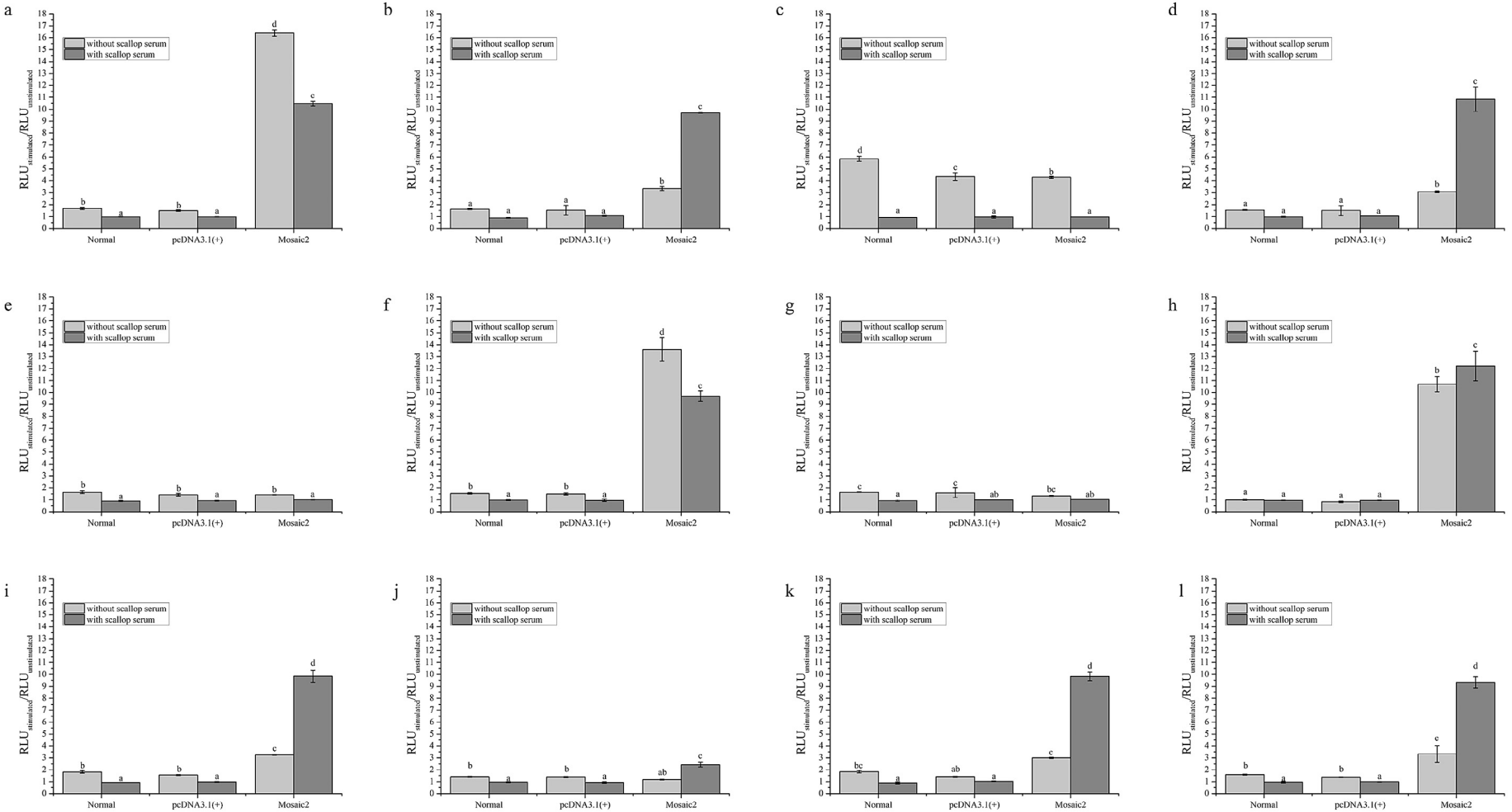

Fig. 5. Ligands for *Cf*TLR. (a) Pam3CSK4, (b) GLU, (c) Zymosa, (d) PGN, (e) Pam2CSK4, (f) poly I:C, (g) LPS, (h) Imiquimod, (i) C-type CpG, (j) D-type CpG, (k) K-type CpG, (l) P-type CpG. Data were normalized to the value of normal group without scallop serum. Vertical bars represented mean ± S.D. (n = 5), and bars with different characters indicated significantly different ($p < 0.05$).

Drosophila (Shi et al., 2009; Wang et al., 2012). Although no Spätzle-like protein has been identified in scallop, some TLR related PAMP binding proteins such as high mobility group box 1 (HMGB1) have already been identified (Wang et al., 2014). Interestingly, the scallop serum could enhance the induction of NFκB in the *Cf*TLR expressing cells elicited by most PAMPs, including GLU, PGN, Imiquimod and four types of CpG, and depress the activation of NFκB luciferase reporter elicited by Pam3CSK4 and poly I:C. The induction and depression effect of scallop serum to the pattern recognition of TLR indicated an existent probability of assistants and competitors to TLR in scallops.

To estimate the effect of ligand properties on pattern recognition by *Cf*TLR, four types of sulphureted CpG were tested in the ligand screening experiment, and the NFκB transactivation in the *Cf*TLR expressing HEK293T cells was found to be induced by C, K and P-type CpG, while the D-type CpG failed to induce NFκB transactivation in *Cf*TLR transfected cells in normal condition. Considering the D-type CpG is different from other types in many properties, such as the intracellular localization and the functional activity (Gursel et al., 2002), this phenomenon could be considered as a direct evidence of the effect of ligand properties on pattern recognition by *Cf*TLR, although the molecular mechanism underlying still waits for further study.

Generally, the pattern recognition ability of TLRs was negatively related to their copy numbers in the genome based on the research achievements of pattern recognition of TLRs from both mammalian and non-mammalian organisms. For example, the TLRs in ascidian (2 TLRs) (Sasaki et al., 2009), mice (12 TLRs) and human (10 TLRs) (Lee et al., 2012) could recognize ligands directly, while the ones from amphioxus (39 TLRs) (Yuan et al., 2009) and oyster (83 TLRs) (Zhang et al., 2015) exhibited no significant pattern recognition ability to ligands. In our current and previous research, only one TLR has been identified from the expressed sequence tags (ESTs), while the other potential sequences were confirmed to be LRR-only proteins in *C. farreri* (Song et al., 2015). So, besides the evolution factors, the copy numbers were suspected to be essentially associated with the pattern recognition ability of TLRs, and even from the hosts in similar evolution position, the TLR with lower copy numbers would have a higher probability in capability of pattern recognition, such as TLRs from scallop and oyster.

In conclusion, the primitive mollusk TLR, *Cf*TLR, was found to develop a hybrid function in pattern recognition with broader ligands, and its mosaic capability of pattern recognition might be due to its basic structure features, ligand properties, and the assistance of some components in scallop serum.

Acknowledgments

We are grateful to all the laboratory members for their technical advices and helpful discussion. This research was supported by National High Technology Research and Development Program (863 Program, No. 2014AA103501 and 2012AA10A401 to Prof. Lingling Wang) from the Chinese Ministry of Science and Technology, and earmarked fund (CARS-48 to Prof. Linsheng Song) for Modern Agro-industry Technology Research System. We also thank Prof. Zhaolan Mo, Yellow Sea Fisheries Research Institute, Chinese Academy of Fishery Sciences, for kindly providing the bacteria *V. anguillarum* strain M3, Prof. Zhenming Chi, College of Marine Life Science, Ocean University of China, for kindly providing the fungi *Y. lipolytica* and Prof. Jiahuai Han, School of Life Sciences, Xiamen University, for kindly providing the plasmids containing the full length cDNA of Human TLR gene.

References

Akira, S., Takeda, K., Kaisho, T., 2001. Toll-like receptors: critical proteins linking innate and acquired immunity. Nat. Immunol. 2, 675–680.
Akira, S., Uematsu, S., Takeuchi, O., 2006. Pathogen recognition and innate immunity. Cell 124, 783–801.
Altschul, S.F., Gish, W., Miller, W., Myers, E.W., Lipman, D.J., 1990. Basic local alignment search tool. J. Mol. Biol. 215, 403–410.
Arts, J.A., Cornelissen, F.H., Cijsouw, T., Hermsen, T., Savelkoul, H.F., Stet, R.J., 2007. Molecular cloning and expression of a Toll receptor in the giant tiger shrimp, *Penaeus monodon*. Fish Shellfish Immunol. 23, 504–513.
Bell, J.K., Mullen, G.E., Leifer, C.A., Mazzoni, A., Davies, D.R., Segal, D.M., 2003. Leucine-rich repeats and pathogen recognition in Toll-like receptors. Trends Immunol. 24, 528–533.
Coscia, M., Giacomelli, S., Oreste, U., 2011. Toll-like receptors: an overview from invertebrates to vertebrates. ISJ-Invert. Surviv. J. 8, 210–226.
Girardin, S.E., Sansonetti, P.J., Philpott, D.J., 2002. Intracellular vs extracellular recognition of pathogens-common concepts in mammals and flies. Trends Microbiol. 10, 193–199.
Guo, Y., Wang, L.L., Zhou, Z., Wang, M.Q., Liu, R., Wang, L.L., et al., 2013. An opioid growth factor receptor (OGFR) for Met^5-enkephalin in *Chlamys farreri*. Fish Shellfish Immunol. 34, 1228–1235.
Gursel, M., Verthelyi, D., Gursel, I., Ishii, K.J., Klinman, D.M., 2002. Differential and competitive activation of human immune cells by distinct classes of CpG oligodeoxynucleotide. J. Leukoc. Bio. 71, 813–820.
Inamori, K., Ariki, S., Kawabata, S., 2004. A Toll-like receptor in horseshoe crabs. Immunol. Rev. 198, 106–115.
Janeway, C.A., Jr., Medzhitov, R., 2002. Innate immune recognition. Annu. Rev. Immunol. 20, 197–216.
Lee, C.C., Avalos, A.M., Ploegh, H.L., 2012. Accessory molecules for Toll-like receptors and their function. Nat. Rev. Immunol. 12, 168–179.
Lemaitre, B., Nicolas, E., Michaut, L., Reichhart, J.-M., Hoffmann, J.A., 1996. The dorsoventral regulatory gene cassette spätzle/Toll/cactus controls the potent antifungal response in *Drosophila* adults. Cell 86, 973–983.
Letunic, I., Doerks, T., Bork, P., 2012. SMART 7: recent updates to the protein domain annotation resource. Nucleic Acids Res. 40, D302–D305.
Leulier, F., Lemaitre, B., 2008. Toll-like receptors-taking an evolutionary approach. Nat. Rev. Genet. 9, 165–178.
Loker, E.S., Adema, C.M., Zhang, S.M., Kepler, T.B., 2004. Invertebrate immune systems-not homogeneous, not simple, not well understood. Immunol. Rev. 198, 10–24.
Matzinger, P., 2002. The danger model: a renewed sense of self. Science 296, 301–305.
Mekata, T., Kono, T., Yoshida, T., Sakai, M., Itami, T., 2008. Identification of cDNA encoding Toll receptor, MjToll gene from kuruma shrimp, *Marsupenaeus japonicus*. Fish Shellfish Immunol. 24, 122–133.
Nyholm, S.V., McFall-Ngai, M., 2004. The winnowing: establishing the squid-*Vibrio* symbiosis. Nat. Rev. Microbiol. 2, 632–642.
O'Neill, L.A., Bowie, A.G., 2007. The family of five: TIR-domain-containing adaptors in Toll-like receptor signalling. Nat. Rev. Immunol. 7, 353–364.
Palm, N.W., Medzhitov, R., 2009. Pattern recognition receptors and control of adaptive immunity. Immunol. Rev. 227, 221–233.
Ren, Q., Zhong, X., Yin, S., Hao, F., Hui, K., Zhang, Z., et al., 2013. The first Toll receptor from the triangle-shell pearl mussel *Hyriopsis cumingii*. Fish Shellfish Immunol. 34, 1287–1293.
Russo, R., Chiaramonte, M., Matranga, V., Arizza, V., 2015. A member of the Tlr family is involved in dsRNA innate immune response in *Paracentrotus lividus* sea urchin. Dev. Comp. Immunol. 51, 271–277.
Sasaki, N., Ogasawara, M., Sekiguchi, T., Kusumoto, S., Satake, H., 2009. Toll-like receptors of the Ascidian *Ciona intestinalis* prototypes with hybrid functionalities of vertebrate toll-like receptors. J. Biol. Chem. 284, 27336–27343.
Shi, X.Z., Zhang, R.R., Jia, Y.P., Zhao, X.F., Yu, X.Q., Wang, J.X., 2009. Identification and molecular characterization of a Spätzle-like protein from Chinese shrimp (*Fenneropenaeus chinensis*). Fish Shellfish Immunol. 27, 610–617.
Song, L.S., Wang, L.L., Zhang, H., Wang, M.Q., 2015. The immune system and its modulation mechanism in scallop. Fish Shellfish Immunol. http://dx.doi.org/10.1016/j.fsi.2015.03.013; In press.
Sun, H.J., Zhou, Z.C., Dong, Y., Yang, A.F., Jiang, B., Gao, S., et al., 2013. Identification and expression analysis of two Toll-like receptor genes from sea cucumber (*Apostichopus japonicus*). Fish Shellfish Immunol. 34, 147–158.
Thompson, J.D., Gibson, T., Higgins, D.G., 2002. Multiple sequence alignment using ClustalW and ClustalX. Curr. Protoc. Bioinformatics Chapter 2:Unit 2.3.
Wang, M.Q., Yang, J.L., Zhou, Z., Qiu, L.M., Wang, L.L., Zhang, H., et al., 2011. A primitive Toll-like receptor signaling pathway in mollusk Zhikong scallop *Chlamys farreri*. Dev. Comp. Immunol. 35, 511–520.
Wang, M.Q., Wang, L.L., Guo, Y., Zhou, Z., Yi, Q.L., Zhang, D.X., et al., 2014. A high mobility group box 1 (HMGB1) gene from *Chlamys farreri* and the DNA-binding ability and pro-inflammatory activity of its recombinant protein. Fish Shellfish Immunol. 36, 393–400.
Wang, P.H., Liang, J.P., Gu, Z.H., Wan, D.H., Weng, S.P., Yu, X.Q., et al., 2012. Molecular cloning, characterization and expression analysis of two novel Tolls (LvToll2 and LvToll3) and three putative Spätzle-like Toll ligands (LvSpz1-3) from *Litopenaeus vannamei*. Dev. Comp. Immunol. 36, 359–371.
Watts, C., 2008. Location, location, location: identifying the neighborhoods of LPS signaling. Nat. Immunol. 9, 343–345.
Wei, Y.C., Pan, T.S., Chang, M.X., Huang, B., Xu, Z., Luo, T.R., et al., 2011. Cloning and expression of Toll-like receptors 1 and 2 from a teleost fish, the orange-spotted grouper *Epinephelus coioides*. Vet. Immunol. Immunopathol. 141, 173–182.
Yang, C.J., Zhang, J.Q., Li, F.H., Ma, H.M., Zhang, Q.L., Jose Priya, T.A., et al., 2008. A Toll receptor from Chinese shrimp *Fenneropenaeus chinensis* is responsive to *Vibrio anguillarum* infection. Fish Shellfish Immunol. 24, 564–574.

Yang, L.S., Yin, Z.X., Liao, J.X., Huang, X.D., Guo, C.J., Weng, S.P., et al., 2007. A Toll receptor in shrimp. Mol. Immunol. 44, 1999–2008.

Yuan, S.C., Huang, S.F., Zhang, W., Wu, T., Dong, M.L., Yu, Y.H., et al., 2009. An amphioxus TLR with dynamic embryonic expression pattern responses to pathogens and activates NF-κB pathway via MyD88. Mol. Immunol. 46, 2348–2356.

Zhang, L.L., Li, L., Zhang, G.F., 2011. A *Crassostrea gigas* Toll-like receptor and comparative analysis of TLR pathway in invertebrates. Fish Shellfish Immunol. 30, 653–660.

Zhang, L.L., Li, L., Guo, X.M., Litman, G.W., Dishaw, L.J., Zhang, G.F., 2015. Massive expansion and functional divergence of innate immune genes in a protostome. Sci. Rep. 5, 8693.

Zhang, Y., He, X.C., Yu, F., Xiang, Z.M., Li, J., Thorpe, K.L., et al., 2013. Characteristic and functional analysis of Toll-like receptors (TLRs) in the lophotrocozoan, *Crassostrea gigas*, reveals ancient origin of TLR-mediated innate immunity. PLoS ONE 8, e76464.